

THE BIRTHRATE AND INITIAL SPIN PERIOD OF SINGLE RADIO PULSARS

RAMESH NARAYAN

Steward Observatory, University of Arizona

Received 1986 November 4; accepted 1987 January 23

ABSTRACT

A statistical analysis of radio pulsar data is presented. Detailed account is taken of known selection effects in pulsar surveys, including the effects of scatter-broadening and period-dependent beaming factor. Two approaches are used: (1) a model-free analysis, based on a V/V_{\max} approach, with large statistical errors; and (2) an analysis based on a luminosity model that leads to much smaller formal errors. Neither approach assumes spin-down by dipole braking. The birthrate of pulsars in the Galaxy is estimated to be one pulsar in ~ 56 yr, and the local rate in the solar neighborhood is estimated to be one pulsar in $\sim 9 \times 10^4$ yr kpc $^{-2}$. The present calculations confirm an earlier result, published by Vivekanand and Narayan in 1981, that many pulsars are born with initial periods as slow as 0.5 s, contrary to the usual belief that initial periods are ~ 10 ms. The pulsars that are born slow typically have high magnetic fields, $\log [B(\text{G})] \gtrsim 12.5$, where B is estimated assuming spin-down through dipole braking. Pulsars that are born fast usually have low fields. Three possibilities are discussed for the correlation between initial spin period and magnetic field: (1) the core of the progenitor star may lose angular momentum to the outer layers through magnetic coupling; (2) the majority of pulsars may be “recycled” through accretion spin-up in binary systems; and (3) the magnetic field may be built up after the neutron star is born, thus delaying the switch-on of a pulsar. If most pulsars are born slow, then their radio emission would be weak at birth, and this might explain why so few pulsars are detected in the centers of supernova remnants.

Subject headings: pulsars — stars: evolution — stars: stellar statistics

I. INTRODUCTION

Ever since their discovery, radio pulsars have been the subject of numerous statistical analyses that have attempted to understand details of their birth, evolution and life history (see Manchester and Taylor 1977; Taylor and Stinebring 1986 for reviews). The earliest such analysis was the celebrated work of Gunn and Ostriker (1970), who with extremely scanty data (31 pulsars known at that time, only 14 with measured period derivatives) made remarkably durable deductions about the distribution and evolution of pulsars. Eight years later, with over 150 pulsars known, Taylor and Manchester (1977) made more reliable calculations. They obtained the distribution of pulsars in the Galaxy and the pulsar luminosity function, and also estimated the birthrate of pulsars in the Galaxy. Their birthrate estimate of one pulsar in ~ 6 yr was, however, a considerable embarrassment since it greatly exceeded the estimated deathrate of massive stars, the supposed progenitors of pulsars. Other independent analyses (e.g., Lyne 1981; Phinney and Blandford 1981) also gave similar estimates for the birthrate.

The above studies neglected a crucial selection effect. The luminosity L of pulsars decreases with increasing period P , and so the mean age of a flux-limited sample of pulsars is significantly lower than that of an unbiased sample. Thus the birthrate estimated from a flux-limited sample tends to be higher than the true value. Vivekanand and Narayan (1981, hereafter VN; see also Narayan and Vivekanand 1981) allowed for this selection effect at the suggestion of J. H. Taylor (1981, private communication). Using an expanded data set that included observations from the Second Molonglo Survey (Manchester *et al.* 1978), VN obtained a new birthrate estimate of one pulsar in ~ 20 yr in the Galaxy.

In the last few years, there have been further developments. It is now recognized that there are several other selection effects that have been neglected in the past. In particular, various factors reduce the ability of pulsar surveys to detect short-period pulsars ($P \lesssim 300$ ms). Also, it now appears that the beaming factor f , which describes the probability that the beam from a randomly oriented pulsar would intersect Earth, may not be a constant ~ 0.2 as thought earlier, but may vary with the pulsar period P , increasing almost to unity for fast pulsars. Further, the distance scale to pulsars has been modified. Including some of these effects, Lyne, Manchester, and Taylor (1985, hereafter LMT) estimated the pulsar birthrate to be one in ~ 50 yr. Here we make an independent estimate of the birthrate, including some effects omitted by LMT, and utilizing a different luminosity model.

The second issue that we focus on concerns the initial spin period, P_i , of radio pulsars. The Crab pulsar, 0531 + 21, is believed to have been born in the supernova explosion of 1054 AD that led to the formation of the Crab Nebula. Because a precise age estimate is available, the life history of this pulsar is known very well, and it is estimated that it was born with an initial period $P_i \approx 16$ ms. The Vela pulsar, 0833–45, in the Vela supernova remnant, and the pulsar, 1509–58, in the remnant, MSH 15–52, are also believed to have been born with P_i of the same order, though with less certainty. The fact that these three youngest known pulsars were all born with short periods has been considered strong evidence that *all* pulsars are born spinning rapidly, with P_i say ~ 10 ms. This assumption was, however, questioned by VN who found from their statistical analysis, after allowing for the dependence of L on P , that the majority of pulsars may be born with P_i of several hundred milliseconds. The result, which VN named “injection” (because pulsars are “injected” at intermediate periods), is surprising if true. If one assumes that main-sequence stars start off rotating rigidly and that they conserve angular momentum locally both during their evolution and during core collapse to a neutron

star, then one expects most pulsars to be born with $P_i \lesssim 1$ ms, close to break-up (e.g. Hardorp 1974). To have $P_i \gtrsim 500$ ms requires that most of the angular momentum should be extracted before, during, or after the collapse. No persuasive agency has been proposed yet to do this.

It is of course possible that VN's analysis missed an important period-dependent selection effect. They did not include the variation of beaming factor f with P , but this acts in the direction of strengthening "injection" since it makes fast pulsars more visible. On the other hand, as mentioned above, there are several other selection effects which make fast pulsars harder to find, and if one of these effects were strong enough it might completely explain "injection." A major motivation for the present study is to check this possibility. All known and suggested P -dependent selection effects have been included in the calculations presented here. Our final conclusion is that these effects are too weak to explain away "injection," and that the majority of pulsars are indeed born with slow periods. Chevalier and Emmering (1986) reached a similar conclusion based on an independent analysis of the pulsar data, as did Srinivasan, Bhattacharya, and Dwarakanath (1984) on the basis of an analysis of plerion statistics.

As further confirmation, we find that there is a marked correlation of P_i with pulsar magnetic field. High field pulsars are born slow much more often than low field pulsars. The fact that "injection" depends on a physical parameter such as the magnetic field appears to further support our contention that "injection" is not due to a statistical fluctuation or selection effect, but is a real physical effect.

Section II of the paper discusses the basic theory behind the present analysis. This is essentially a recapitulation of the techniques developed by VN. Section III considers in detail all the selection effects of the major pulsar surveys, paying particular attention to those that depend on pulsar period. Section IV discusses the issue of a luminosity model for radio pulsars. The model of LMT, which was based on the work of Gunn and Ostriker (1970), is rejected in favor of a power-law model, which fits the data better. Section V describes the numerical results of the analysis, and § VI discusses their significance.

A preliminary version of the present work was reported in Narayan (1987).

II. THEORY

We make the standard assumption that the pulsar distribution in the Galaxy can be written as a continuous function and that it can be factored in the form

$$\rho(R, z, P, \dot{P}, L) 2\pi R dR dz dP d\dot{P} dL = [\rho_R(R) 2\pi R dR] [\rho_z(z) dz] [\rho_t(P, \dot{P}, L) dP d\dot{P} dL], \quad (2.1)$$

where R is the galactocentric radius, z is height above the Galactic plane, P is the pulsar period, \dot{P} is the time derivative of P , and L is the pulsar luminosity. We normalize $\rho_R(R)$ and $\rho_z(z)$ so that the integrals over Galactic coordinates give unity. Thus, the function $\rho_t(P, \dot{P}, L)$ (where t stands for "true") describes the smoothed pulsar distribution that would be obtained if one could detect every pulsar in the Galaxy. The factorization assumed in equation (2.1) is only approximately valid since pulsars are born in the Galactic plane and move to higher z as they age. In fact, it is known that there is a positive correlation between the z -height of a pulsar and its period P , as well as its characteristic age τ , defined by

$$\tau = P/2\dot{P}. \quad (2.2)$$

Hence, $\rho_t(P, \dot{P}, L)$ cannot be independent of z . However, we believe that the error introduced by this simplification is not serious, as discussed in § VI.

The luminosity L of a pulsar at distance d from Earth can be expressed in the form

$$L = Sd^2, \quad (2.3)$$

where S is the radio flux received at Earth in a particular wavelength band. Following Taylor and Manchester (1977), we deal exclusively with L at 400 MHz, and express it in the practical units of mJy kpc².

We restrict our attention in this paper to the pulsars detected by four major 400 MHz radio surveys: Jodrell Bank Survey (Davies, Lyne, and Seiradakis 1972), U Mass-Arecibo Survey (Hulse and Taylor 1974), Second Molongo Survey (Manchester *et al.* 1978), and U Mass-NRAO Survey (Damashek, Taylor, and Hulse 1978). Recently, there have been other surveys at 400 MHz with improved sensitivity for pulsars with low luminosities and short periods: Princeton-NRAO Survey, Phase I (Dewey *et al.* 1985), Phase II (Stokes *et al.* 1985), Princeton-Arecibo Survey (Segelstein *et al.* 1986). However, no period derivatives have been published for the new pulsars discovered, and therefore we are not in a position to include these surveys in our calculations.

Let us describe the pulsars detected by the four surveys by means of a smooth distribution $\rho_o(P, \dot{P}, L)$ (where o stands for "observed"). This function is related to the true distribution $\rho_t(P, \dot{P}, L)$ by two factors:

1. The solid angle swept out by the beam of a spinning pulsar is only a fraction of 4π . The mean pulse duty cycle of pulsars is $\sim 4\%$, which implies a beam half-power-width in the "east-west" direction (defined with respect to the rotation axis) of order $\sim 14^\circ$. If the unknown north-south width is taken to be the same, and if the orientations of the rotation and magnetic axes are random in space, then the beaming factor f (= solid angle swept by pulsar beam/ 4π) will be $f \approx 0.2$ (Gunn and Ostriker 1970). However, several recent studies indicate that pulsar beams are elongated in the meridional direction (Narayan and Vivekanand 1982, 1983a, b; Narayan and Radhakrishnan 1983; see Narayan 1984 for a summary). Moreover, it seems that the ratio R of the NS to EW dimensions of the beam varies with pulsar period P as (Narayan and Vivekanand 1983b)

$$R \approx 1.8P^{-0.6}. \quad (2.4)$$

Thus, the beaming factor f is a function of P , with the variation shown in Figure 1. Note that $f(P) > 0.2$ over most of the range of pulsar periods. In fact, at short periods $\lesssim 0.1$ s, $f(P) \approx 1$ in this model, which means that fast pulsars are potentially visible from all directions.

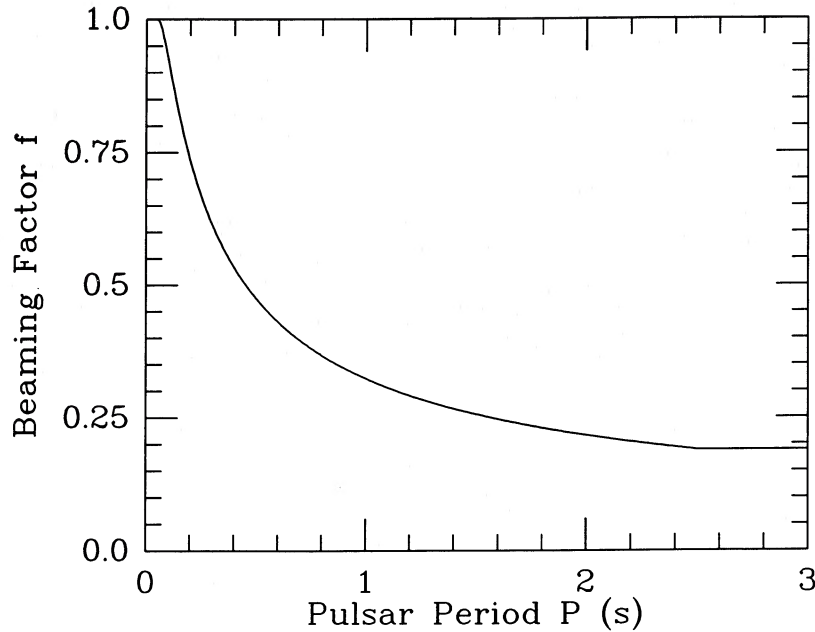


FIG. 1.—Variation of the beaming factor f with pulsar period P for the beam elongation model of eq. (2.4) (Narayan and Vivekanand 1983b). The rotation and magnetic axes of the pulsar are assumed to be randomly oriented.

2. Even if the beam points toward Earth, a pulsar would not be detected if it were fainter than the minimum detection limit of pulsar surveys, or if it were in a direction that has not been searched. We allow for this by introducing the following scale factor:

$$\mathcal{S}(P, L) = \frac{\iint \rho_R(R) \rho_z(z) R dR d\Phi dz}{\iint' \rho_R(R) \rho_z(z) R dR d\Phi dz} \quad (2.5)$$

where the integral \iint in the numerator is over the whole Galaxy (Φ is galactocentric azimuthal angle), while the integral \iint' in the denominator is over only that part of the Galaxy where a pulsar with period P and luminosity L could have been detected by at least one of the four surveys included in the calculation. The computation of $\mathcal{S}(P, L)$ including all selection effects is somewhat involved, and we defer a discussion of it to § III. Note that $\mathcal{S}(P, L)$ is related to the classic V/V_{\max} ratio; in fact $[\mathcal{S}(P, L)]^{-1}$ is equal to a weighted V/V_{\max} , where the weight is the space density of pulsars in the Galaxy.

Using the above two factors, we can now write

$$\rho_i(P, \dot{P}, L) dP d\dot{P} dL = [\mathcal{S}(P, L) f(P)] \rho_o(P, \dot{P}, L) dP d\dot{P} dL. \quad (2.6)$$

The total number of active single pulsars in the Galaxy is then estimated to be

$$N_{\text{psr}} = \iiint \rho_i(P, \dot{P}, L) dP d\dot{P} dL = \iiint [\mathcal{S}(P, L) f(P)] \rho_o(P, \dot{P}, L) dP d\dot{P} dL \approx \sum_i \mathcal{S}(P_i, L_i) f(P_i). \quad (2.7)$$

The final sum is obtained by replacing the smooth distribution function $\rho_o(P, \dot{P}, L)$ by the actual pulsars detected by the four surveys with radio flux above the modeled minimum sensitivity limits of the surveys. Since we are interested in only *single* pulsars in this paper, binaries are excluded from consideration in the calculations.

Consider now the *current* of pulsars, $J(P)$, a useful quantity introduced by Phinney and Blandford (1981) and VN. This is defined to be the number of pulsars crossing per unit time from periods shorter than P to longer than P , i.e.,

$$J(P) = \iint \dot{P} \rho_i(P, \dot{P}, L) d\dot{P} dL. \quad (2.8)$$

To improve the statistics, it is more convenient to consider the average current in a period-interval, defined as

$$\begin{aligned} \bar{J}(P_1, P_2) &= \frac{1}{(P_2 - P_1)} \int_{P_1}^{P_2} J(P) dP \\ &= \frac{1}{(P_2 - P_1)} \int_{P_1}^{P_2} \iint \dot{P} \left[\frac{\mathcal{S}(P, L)}{f(P)} \right] \rho_o(P, \dot{P}, L) d\dot{P} dL dP \\ &\approx \frac{1}{(P_2 - P_1)} \sum_i' \frac{\dot{P}_i \mathcal{S}(P_i, L_i)}{f(P_i)}, \end{aligned} \quad (2.9)$$

where the summation \sum' is restricted to pulsars with period P lying in the range between P_1 and P_2 detected by the various surveys.

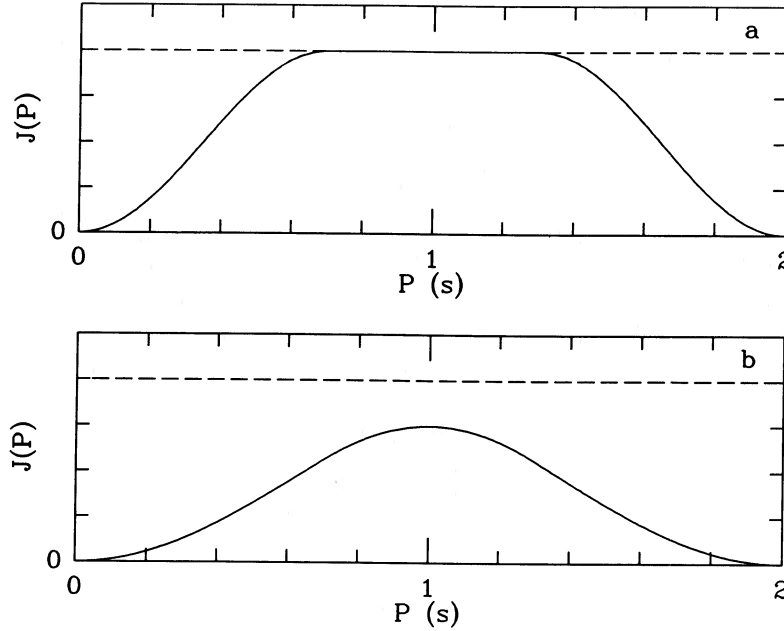


FIG. 2.—(a) Schematic variation of the “current” $J(P)$ with P for a case where all pulsars are born with initial period $P < P_b = 0.7$ s and die with $P > P_d = 1.3$ s. The current equals the birthrate BR_{tot} , shown by the dashed line, for the period range $P_b < P < P_d$. (b) A case where $P_b = 1.3$ s is greater than $P_d = 0.7$ s. Here $J(P)$ lies below BR_{tot} over the whole range of P .

In steady state, $J(P)$ measures the birthrate minus the deathrate of pulsars with period less than P , i.e.,

$$J(P) = \int_0^P [\text{BR}(P) - \text{DR}(P)] dP, \quad (2.10)$$

where $\text{BR}(P)$ and $\text{DR}(P)$ are *differential* birthrates and deathrates per unit interval of P . Let all pulsars be born with $P_i < P_b$ and die with $P > P_d$. Figure 2 shows two possible cases. If $P_d > P_b$ (Fig. 2a), then, between the periods P_b and P_d , $J(P)$ is equal to the total pulsar birthrate BR_{tot} ,

$$BR_{tot} \equiv \int_0^{P_b} \text{BR}(P) dP = \bar{J}(P_b, P_d). \quad (2.11)$$

This case is unlikely to be rigorously true in practice. For instance, the 1.5 ms pulsar, 1937+21, will almost certainly switch off before reaching the initial period, $P_i \approx 16$ ms, of the Crab pulsar. If $P_d < P_b$ (Fig. 2b), then all we have is a bound on BR_{tot} , i.e.,

$$BR_{tot} \geq \bar{J}(P_1, P_2), \quad (2.12)$$

for any P_1, P_2 . Fortunately, as we show later, the pulsar birthrate is dominated by a class of high magnetic field pulsars. Therefore, if we choose P_b and P_d corresponding to these, the birthrate we estimate would fall short of the true value by only a small amount, and we could use \bar{J} directly as an estimate of the total birthrate.

It should be emphasized that the estimate of birthrate obtained through pulsar current makes no assumption at all regarding the mechanism of pulsar spin-down. We consider this a major improvement over other approaches, which invariably need to assume dipole braking.

III. COMPUTATION OF THE SCALE FACTOR $\mathcal{S}(P, L)$

As shown in equation (2.5), the computation of the scale factor $\mathcal{S}(P, L)$ involves integrals over the galactic density functions $\rho_R(R)$, $\rho_z(z)$. LMT, following the iterative methods of Large (1971), used recent data to obtain histograms of $\rho_R(R)$ and $\rho_z(z)$. The radial density function, shown in Figure 3a, appears to have a deficit of pulsars near the Galactic center, for $R \approx 5$ kpc. (The Sun is assumed to be at $R = 10$ kpc in these calculations.) However, it is not clear that this is a real effect since scatter-broadening drastically reduces the visibility of pulsars in this region of the Galaxy at 400 MHz. A recent 1400 MHz survey by Clifton and Lyne (1986) detected many new pulsars near the Galactic center, and the deficit may be less than supposed earlier. To keep matters simple, we fit a simple Gaussian to the data. This gives the normalized function

$$\rho_R(R) = \frac{1}{64\pi} \exp \left[- \left(\frac{R}{8} \right)^2 \right] (\text{kpc})^{-2}, \quad (3.1)$$

where R is in kpc. [An exponential model may be preferable since the progenitors of pulsars are Population I stars in the Galaxy; however, it makes no difference for this paper since the results are quite insensitive to the precise functional form of $\rho_R(R)$.] Figure 3b

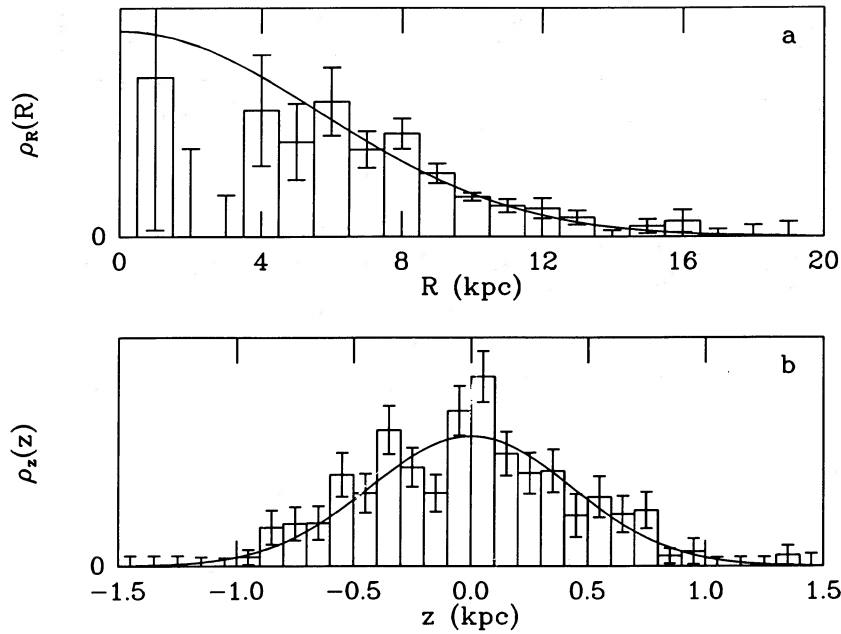


FIG. 3.—(a) The histogram shows the radial pulsar density, $\rho_R(R)$, estimated by LMT (1985). The smooth curve is the best-fit Gaussian, described by eq. (3.1). (b) Histogram of $\rho_z(z)$, estimated by LMT. The smooth curve is the best-fit Gaussian, described by equation (3.2).

shows the histogram in z estimated by LMT, and this is again fitted to a Gaussian to give

$$\rho_z(z) = \frac{1}{0.61\pi^{1/2}} \exp\left[-\left(\frac{z}{0.61}\right)^2\right] (\text{kpc})^{-2}. \quad (3.2)$$

With the above normalizations, the numerator of equation (2.5) gives unity.

To calculate the denominator of equation (2.5), we need detailed models of the sensitivities of the four surveys included in the calculation. Dewey *et al.* (1984) give the following general formula for the minimum detection flux S_{\min} of a survey (see also Vivekanand, Narayan, and Radhakrishnan 1982)

$$S_{\min} = \beta S_o \left(\frac{T_r + T_{\text{sky}}}{T_o} \right) \left[\frac{PW}{W_e(P - W)} \right]^{1/2} \text{ mJy}. \quad (3.3)$$

This formula is to be used over the region of sky covered by each survey. T_r is the receiver excess noise temperature, T_{sky} is the sky background temperature at the longitude l and latitude b of the particular line-of-sight, and T_o is a suitable normalization constant. W_e is the equivalent width of the unbroadened pulse, and W is the measured pulse width, given by

$$W^2 = W_e^2 + \tau_{\text{samp}}^2 + \tau_{\text{DM}}^2 + \tau_{\text{scatt}}^2, \quad (3.4)$$

where τ_{samp} is the broadening caused by the finite sampling time of the data, τ_{DM} is due to dispersion smearing, and τ_{scatt} is due to scatter-broadening. S_o (mJy) is the minimum detection limit for a pulsar in the center of the telescope beam in the ideal situation when $W = W_e \ll P$ and $T_{\text{sky}} \ll T_r$. Since pulsar surveys usually cover the sky in overlapping steps, there is a loss of efficiency for regions of sky that are off-center, and the factor β allows for this. In the case of the Second Molongo Survey, the observations were conducted such that a constant length of data was analyzed for declinations $\delta < 30^\circ$, and twice that length was analyzed for $\delta > 30^\circ$. This introduces an extra factor of $1/2^{1/2}$ in equation (3.3) for $\delta > 30^\circ$.

Table 1 lists the various details of the four surveys, including the sky coverage and values of T_r and T_o . The data have been taken

TABLE 1
PARAMETERS OF THE JODRELL BANK, U MASS-ARECIBO, SECOND MOLONGLO,
AND U MASS-NRAO SURVEYS

Parameter	Jodrell	Arecibo	Molongo	NRAO
Sky coverage	$-8^\circ < l < 115^\circ$ $ b < 7^\circ$	$42^\circ < l < 60^\circ$ $ b < 4^\circ$	$-85^\circ < \delta < 20^\circ$	$\delta > 20^\circ$
T_r (K)	110	110	210	170
T_o (K)	140	260	240	200
τ_{samp} (ms)	80	33	40	33
C_{DM}	3.0×10^{-4}	9.4×10^{-6}	$6.0 \times 10^{-5}, b < 18^\circ$ $3.0 \times 10^{-4}, b > 18^\circ$	1.5×10^{-4}
βS_o (mJy)	10	2	8	12

from Dewey *et al.* (1984) and LMT, and from the original papers. Manchester and Taylor (1981) list T_{sky} at 400 MHz for 330 pulsars. For the more recently discovered pulsars, we obtained T_{sky} from the 408 MHz all-sky map published by Haslam *et al.* (1982). Using these estimates, the variation of T_{sky} with l and b (both expressed in degrees, with $|l| \leq 180^\circ$) was fitted to obtain the following simple model:

$$T_{\text{sky}}(l, b) = 25 + 275/[1 + (l/42)^2][1 + (b/3)^2]. \quad (3.5)$$

The form of the model is identical to the one used by Taylor and Manchester (1977), but the parameters differ slightly.

We assume that all pulsars have an intrinsic duty cycle of 4%, and hence we take

$$W_e = 0.04P. \quad (3.6)$$

The values of τ_{samp} were taken from Dewey *et al.* (1984) and are listed in Table 1.

The dispersion broadening τ_{DM} is of the form

$$\tau_{\text{DM}} = C_{\text{DM}} \text{DM}, \quad (3.7)$$

where DM is the dispersion measure (units: $\text{cm}^{-3} \text{ pc}$) of a given pulsar, and C_{DM} is a constant, listed in Table 1, that depends on the details of each survey. For any potential location of a pulsar in the Galaxy, DM is given by the following integral

$$\text{DM} = 10^3 \int_0^d n_e(l) dl \text{ pc cm}^{-3},$$

where $n_e(l)$ is the free electron density at distance l (kpc) along the line of sight to the pulsar, and d (kpc) is the total distance to the pulsar. We used the following model of LMT for the electron density at galactocentric coordinates R, z , (kpc):

$$n_e(R, z) = \left[0.025 + 0.015 \exp\left(-\frac{|z|}{0.07}\right) \right] \left[\frac{2}{1 + R/10} \right] \text{ cm}^{-3}. \quad (3.8)$$

The scatter-broadening τ_{scatt} can be written in the form (Romani, Narayan, and Blandford 1986)

$$\begin{aligned} \tau_{\text{scatt}} &= 2.9 \times 10^{-3} (10^4 C_N^2)^{6/5} \lambda^{22/5} d^{11/5} \text{ ms} \\ &= 52 (C_N^2)^{6/5} d_{\text{kpc}}^{11/5} \text{ ms} \quad (\text{at } 400 \text{ MHz}), \end{aligned} \quad (3.9)$$

where the distance d to the pulsar is in kpc, the radio wavelength λ of the survey is in meters, and $C_N^2 (m^{-20/3})$ is a parameter that describes the mean electron density fluctuation power δn_e^2 in the line of sight (e.g., Rickett 1978). Cordes, Weisberg, and Boriakoff (1984) have shown that there is a smooth component of C_N^2 in the Galaxy with a constant value, $\log(C_N^2) = -3.5$, and an additional clumpy component, restricted to $|z| < 0.1$ kpc, that peaks in the inner region of the Galaxy. Assuming that the second component is also smoothly distributed, we can approximately write

$$C_N^2 = 10^{-3.5} + \frac{1}{d} \int_0^d C_{\text{scatt}}(l) dl m^{-20/3}, \quad (3.10)$$

where $C_{\text{scatt}}(l)$ is proportional to δn_e^2 of the second component at distance l along the line of sight. We have modeled this δn_e^2 to be a Gaussian as a function of galactocentric radius R (kpc) and optimized its normalization constant and scale length by means of a least-squares fit to the measured C_N^2 listed by Cordes, Weisberg, and Boriakoff (1984). We then obtain the following model for C_{scatt}

$$\begin{aligned} C_{\text{scatt}}(R, z) &= 6.8 \exp[-(R/3.5)^2] m^{-20/3}, & |z| \leq 0.1 \text{ kpc} \\ &= 0, & |z| > 0.1 \text{ kpc}. \end{aligned} \quad (3.11)$$

This model gives $\log(C_N^2) \approx -3.5$ for nearby pulsars, and $\log(C_N^2) \geq 0$ for pulsars in the inner Galaxy, consistent with the data.

The only parameter remaining in equation (3.3) is βS_0 , which was determined as follows. For each survey, a reduced flux S_{red} was calculated for every pulsar detected by that survey (compare with eq. [3.3]),

$$S_{\text{red}} = S \left/ \left(\frac{T_r + T_{\text{sky}}}{T_0} \right) \left[\frac{PW}{W_e(P - W)} \right]^{1/2} \right. \text{ mJy}, \quad (3.12)$$

where S is the actual measured flux. (In the case of the Second Molonglo Survey alone there is an additional factor of $2^{1/2}$ for $\delta > 30^\circ$ as discussed earlier.) A histogram of S_{red} has a peak at some intermediate value of S_{red} . The fall-off above the peak is due to the steep pulsar luminosity function (bright pulsars are much rarer than faint ones). The fall-off below the peak is because of the sensitivity limit of the survey. An approximate estimate of βS_0 can be obtained by selecting a value of S_{red} near the peak (see Vivekanand, Narayan, and Radhakrishnan 1982). Figure 4 shows the results for the four surveys considered here, and the corresponding values of βS_0 are listed in Table 1.

The scale factors $\mathcal{S}(P, L)$ were now computed over a grid in P and L using equation (2.5) by means of a Monte Carlo scheme. A point was selected at random in the Galaxy, and the numerator, which can be thought of as a weighted total volume, V_{max} , was updated by adding the weight $\rho_R(R)\rho_z(z)$ to it. For the denominator, the pulsar flux $S = L/d^2$ was computed and for each P , the value of $S_{\text{min}}(P)$ was calculated for the four surveys. If S was greater than S_{min} for any of the surveys, then the denominator, which is like a weighted volume, $V(P, L)$, was updated by adding $\rho_R(R)\rho_z(Z)$. This was done for all P, L in the grid. By repeating for a large

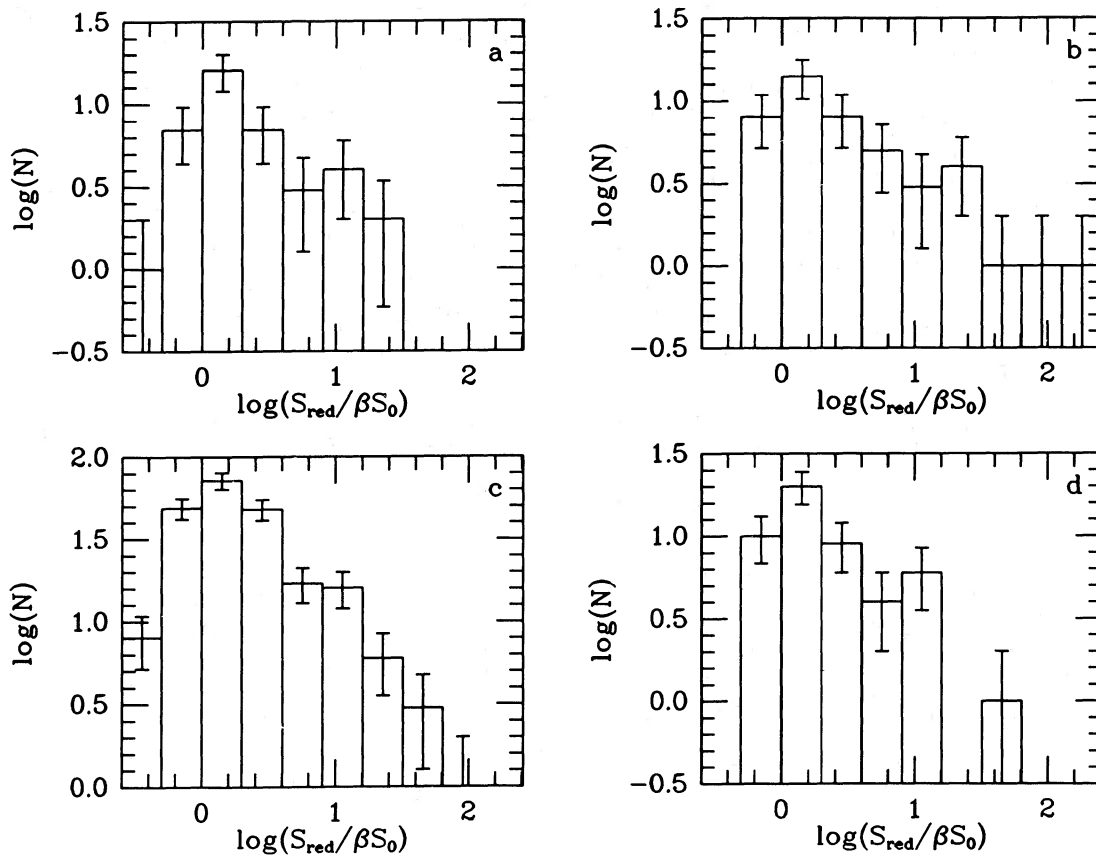


FIG. 4.—(a) Histogram of $S_{\text{red}}/\beta S_0$ for all pulsars detected in the Jodrell Bank Survey (Davies *et al.* 1972); βS_0 is taken to be 10 mJy. (b) U Mass-Arecibo Survey (Hulse and Taylor 1974), $\beta S_0 = 2$ mJy. (c) Second Molonglo Survey (Manchester *et al.* 1978), $\beta S_0 = 8$ mJy. (d) U Mass-NRAO Survey (Damashek *et al.* 1978), $\beta S_0 = 12$ mJy.

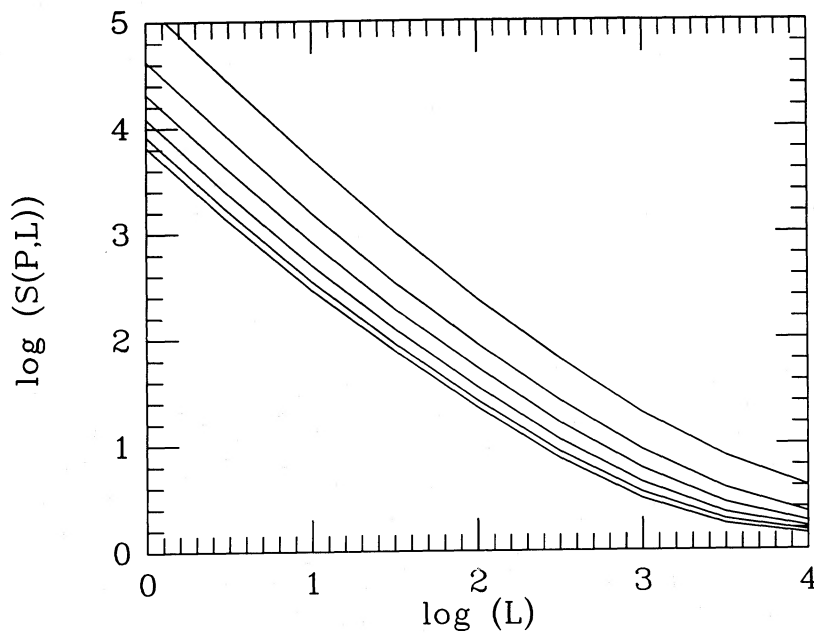


FIG. 5.—Variation of $\log \mathcal{S}(P, L)$ with $\log L$. Starting from the top, the curves correspond to $P = 0.05$ s, 0.1 s, 0.2 s, 0.4 s, 0.8 s, 1.6 s.

number of random pulsar positions in the Galaxy, approximations of V_{\max} and $V(P, L)$ were obtained. Finally, the scale factors were calculated as

$$\mathcal{S}(P, L) = V_{\max}/V(P, L) . \tag{3.13}$$

Since the majority of pulsars are weak and are detected only when they happen to be physically close to the Sun, the Monte Carlo scheme was arranged so that the volume of the Galaxy near the Sun was sampled much more often than distant parts of the Galaxy. The weights used in evaluating V_{\max} and $V(P, L)$ were reduced by the oversampling factor in this region to compensate for this.

Figure 5 shows the variation of $\mathcal{S}(P, L)$ with P and L . There are two trends. First, $\mathcal{S}(P, L)$ is very large at low values of L and tends to ~ 1 for high L . This reflects the variation with L of the effective Galactic volume surveyed and emphasizes the point that faint pulsars are much more important for statistical studies than bright ones. Second, $\mathcal{S}(P, L)$ increases dramatically at short P , below a few hundred ms. This is because of the various period-dependent selection effects that go into the expression for the pulse width W in equation (3.4).

In order to use the table of $\mathcal{S}(P, L)$ it is important to restrict our attention to the subset of pulsars that were detected by the four major surveys with flux S greater than the modeled S_{\min} (eq. [3.3]). When this criterion is applied, the list of single pulsars consists of 220 objects. We have calculated $\mathcal{S}(P, L)$ (needed in eq. [2.7]) and $\dot{P}\mathcal{S}(P, L)$ (needed in eq. [2.9]) for these pulsars (except in a few cases where \dot{P} is unmeasured). Figure 6 shows histograms of the distributions of these quantities. The long tail at high values of $\dot{P}\mathcal{S}(P, L)$ is disturbing. It implies that an estimate of birthrate obtained using \bar{J} as defined in equation (2.9) will have low statistical reliability because, although we have 220 pulsars in our data base, the *effective* number of pulsars that contribute to our birthrate estimate is very small, possibly as small as 2 or 3.

IV. LUMINOSITY MODEL AND THE SCALE FACTOR $\mathcal{A}(P, \dot{P})$

The theory of § II and the scale factor $\mathcal{S}(P, L)$ are valid for general ρ_o and ρ_t that are arbitrary functions of P, \dot{P} , and L . Because of this generality, the theory is highly model-independent, but it also leads to poor statistics. In this section we introduce extra information in the form of a model for pulsar radio luminosity. The statistical significance of the results is thus greatly improved, though at the risk of introducing systematic errors.

Lyne, Ritchings, and Smith (1975) showed that the luminosity L of a pulsar is not independent of P and \dot{P} , but in fact has a power-law dependence on these parameters. This has been confirmed in later work by VN and Proszynski and Przybicien (1984). These studies showed that the correlation is statistically very significant and, although they used different data sets, all the studies obtained similar values for the power-law exponents. Rounding off the exponents, we write the model pulsar luminosity L_m for a given P and \dot{P} as

$$\log L_m = 1.72 + [\log (\dot{P}_{-15}/P^3)]/3 , \tag{4.1}$$

where L_m is in units of mJy kpc² and $\dot{P}_{-15} = 10^{15}\dot{P}$. Figure 7 shows the agreement between this model and the observed luminosities of pulsars, grouped in bins of 30 pulsars each. The χ^2 of the fit is 10, which is acceptable.

Apart from the good fit, a model in which the radio luminosity L_m depends on \dot{P}/P^3 is appealing for two reasons. First, \dot{P}/P^3 is

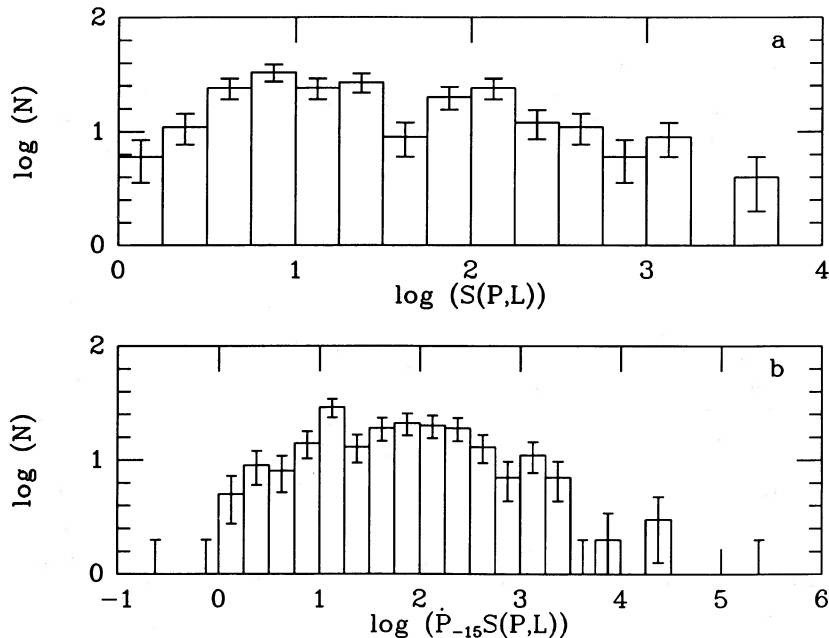


FIG. 6.—(a) Histogram of $\mathcal{S}(P, L)$ corresponding to the 220 pulsars included in the calculations. (b) Histogram of $\dot{P}_{-15}\mathcal{S}(P, L)$ for 204 of the 220 pulsars for which $\dot{P}_{-15} \equiv 10^{15}\dot{P}$ is available.

1987ApJ...319...162N

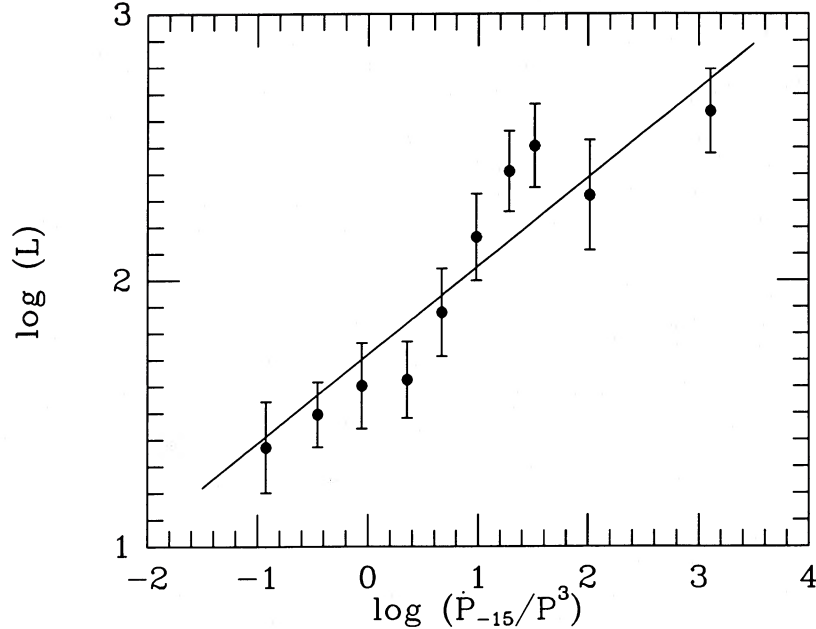


FIG. 7.—The luminosity model, eq. (4.1), compared to the data

proportional to L_{tot} , the rate of loss of total rotational energy of the pulsar. Second, pulsars seem to switch off in the radio when \dot{P}/P^3 falls below a critical value $\sim 10^{-16} \text{ s}^{-3}$ (Taylor and Stinebring 1986), and it is satisfying to have L_m depend on this quantity.

Gunn and Ostriker (1970) originally proposed a different luminosity model, viz.,

$$L_m \propto B^2, \quad (4.2)$$

where B , the pulsar magnetic field, is estimated assuming dipole spin-down torque,

$$B \sim 10^{12}(P\dot{P}_{-15})^{1/2} \text{ G}. \quad (4.3)$$

LMT used this model in their work. While the model may be physically plausible, it agrees rather poorly with the data. We prefer to use the model of equation (4.1) in our calculations.

Although equation (4.1) is a good representation of the variation of mean luminosity with P , \dot{P} , there is a very large dispersion of L around this mean. We allow for this by factoring the observed pulsar distribution in the form

$$\rho_o(P, \dot{P}, L)dPd\dot{P}dL = [\rho_o(P, \dot{P})dPd\dot{P}][\rho_L(\log L - \log L_m)d \log L], \quad (4.4)$$

where ρ_L is normalized so that it integrates to unity. The crucial assumption here is that the distribution of $(\log L - \log L_m)$ is independent of P , \dot{P} , which is reasonable since the dispersion of $\log L$ around the mean is remarkably constant for the different bins in Figure 7. The shape of the function ρ_L is shown by the histogram in Figure 8, which combines the data on all pulsars. The distribution is quite symmetric around the mean, and we model it by means of the following function

$$\begin{aligned} \rho_L(\log L - \log L_m) &= 0.2144\{1 + \cos [1.347(\log L - \log L_m)]\}, & |\log L - \log L_m| \leq 2.332 \\ &= 0, & |\log L - \log L_m| > 2.332. \end{aligned} \quad (4.5)$$

The fit, shown in Figure 8, is good.

The advantage with the factored form of equation (4.4) is that instead of requiring the set of observed pulsars to describe the *three-dimensional* function $\rho_o(P, \dot{P}, L)$ as in §§ II and III, we now require it to describe only the *two-dimensional* function $\rho_o(P, \dot{P})$. The dependence on L is taken care of through the luminosity model, equations (4.1) and 4.5). Statistically speaking, the results from this scheme should be far more reliable than with the earlier scheme. However, there is a greater danger of systematic errors creeping in from inadequacies in the luminosity model.

Equation (2.8) now becomes modified to

$$\begin{aligned} J(P) &= \iint \dot{P}[\mathcal{S}(P, L)/f(P)]\rho_o(P, \dot{P}, L)d\dot{P}dL \\ &= \int \dot{P}[\mathcal{S}(P, \dot{P})/f(P)]\rho_o(P, \dot{P})d\dot{P}, \end{aligned} \quad (4.6)$$

where we have defined a new scale factor

$$\mathcal{S}(P, \dot{P}) \equiv \int \mathcal{S}(P, L)\rho_L[\log L - \log L_m(P, \dot{P})]d \log L. \quad (4.7)$$

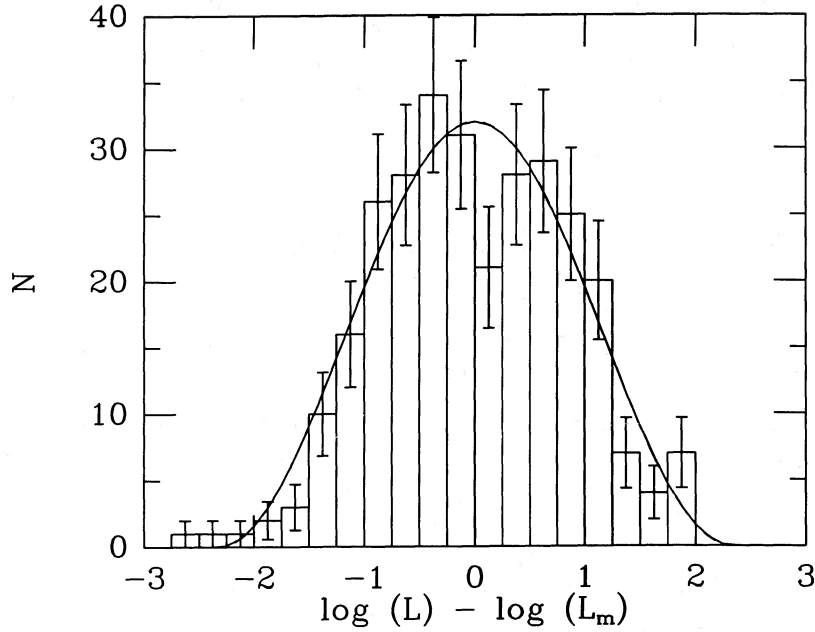


FIG. 8.—The histogram shows the distribution of $\log L$ around the model luminosity $\log L_m$. The smooth curve corresponds to eq. (4.5).

The average current in a period-interval is now

$$\bar{J}(P_1, P_2) \approx \frac{1}{(P_2 - P_1)} \sum_i \frac{P_i \mathcal{S}(P_i, \dot{P}_i)}{f(P_i)}, \quad (4.8)$$

where, as before, the summation is restricted to pulsars with $P_1 \leq P \leq P_2$. Similarly, N_{psr} is obtained by substituting $\mathcal{S}(P_i, \dot{P}_i)$ for $\mathcal{S}(P_i, L_i)$ in equation (2.7).

Figure 9 shows histograms of the distributions of $\mathcal{S}(P, \dot{P})$ and $\dot{P} \mathcal{S}(P, \dot{P})$. Note that these histograms are much more compact than those in Figure 6, which makes a profound difference in the statistics.

It should be noted that although we have introduced a pulsar luminosity model in this section, we still have not assumed anything regarding the nature of pulsar spin-down.

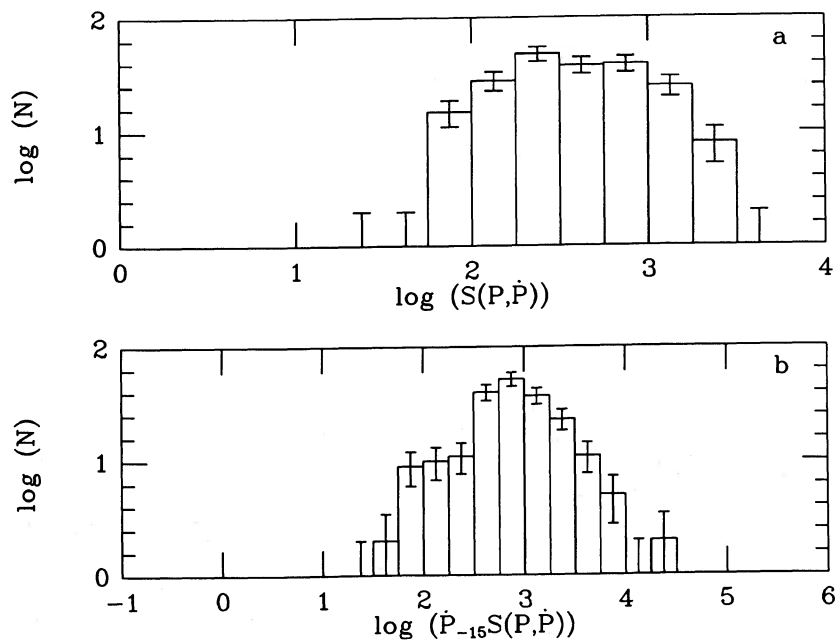


FIG. 9.—(a) Histogram of $\mathcal{S}(P, \dot{P})$. (b) Histogram of $\dot{P}^{-15} \mathcal{S}(P, \dot{P})$.

V. RESULTS

It was seen in § II that there are two models for the beaming factor: (1) a constant factor, $f = 0.2$; and (2) a variable factor, $f(P)$, with the variation shown in Figure 1. Substituting these in equation (2.7), and using the list of 220 single pulsars detected by the four surveys with $S \geq S_{\min}$, we estimate the total number of pulsars in the Galaxy to be

$$f = f(P): \quad N_{\text{psr}} = (1.46 \pm 0.34) \times 10^5, \quad (5.1)$$

$$f = 0.2: \quad N_{\text{psr}} = (2.35 \pm 0.48) \times 10^5, \quad (5.2)$$

The error estimates correspond to 1 σ deviations, σ_N , and were estimated by (see VN)

$$\sigma_N^2 \approx \sum_i [\mathcal{S}(P_i, L_i)/f(P_i)]^2. \quad (5.3)$$

Note that the estimate of N_{psr} using $f(P)$ is less than that using $f = 0.2$. The bulk of the contribution to N_{psr} comes from pulsars with $P \approx 0.7$ –1 s. As seen in Figure 1, $f(P)$ for these pulsars is ~ 0.3 –0.4, and so the ratio is ~ 1.5 –2. A similar ratio carries through in birthrate estimates as well.

A problem with the above estimate of N_{psr} is that the observed sample of pulsars is mostly clustered near the Sun, and we need to assume a functional form for $\rho_R(R)$ in order to extrapolate to the whole Galaxy. As discussed in § III, $\rho_R(R)$ is not known well in the inner part of the Galaxy, and, in particular, it is not clear whether $\rho_R(R)$ cuts off for $R \lesssim 5$ kpc. Due to this uncertainty, it is worthwhile to estimate a *local* number density of pulsars in the solar vicinity. Such a number would be much more reliable, and, as emphasized by Blaauw (1985), it would be easier to make a comparison with the number density of pulsar progenitors such as massive stars, since these too are detected only in the solar vicinity.

To compute the local number density, we restricted our attention to a square area in the Galactic disk of side 2 kpc, centered on the Sun. We computed scale factors $S_{\text{loc}}(P, L)$ for this volume by restricting the R and Φ integrations in equation (2.5) to this range. We also truncated the earlier list of 220 pulsars to a new list of 62 pulsars that lie within the (2×2) kpc square. The areal density of pulsars in the solar vicinity is then given by

$$N_{\text{loc}} \approx \frac{1}{4} \sum_i S_{\text{loc}}(P_i, L_i)/f(P_i) \text{ kpc}^{-2}, \quad (5.4)$$

where the factor of $\frac{1}{4}$ is to convert from an area of 4 kpc^2 to 1 kpc^2 , and the summation is over the shortened list of 62 pulsars. We thus obtain

$$f = f(P): \quad N_{\text{loc}} = 152 \pm 35 \text{ kpc}^{-2}, \quad (5.5)$$

$$f = 0.2: \quad N_{\text{loc}} = 243 \pm 50 \text{ kpc}^{-2}. \quad (5.6)$$

Comparing with equations (5.1), (5.2), we see that the effective area of the Galaxy is

$$A_{\text{eff}} \approx 10^3 \text{ kpc}^2. \quad (5.7)$$

This is the area that would be occupied if all the pulsars in the Galaxy were spread out into a uniform sheet with number density equal to the solar value. The precise value of A_{eff} depends on the model used for $\rho_R(R)$.

Coming now to pulsar current and birthrate, we note that, in addition to the two models for f , there are also two models for the scale factor, viz., $\mathcal{S}(P, L)$ (§ III) and $\mathcal{S}(P, \dot{P})$ (§ IV). [We did not need to introduce $\mathcal{S}(P, \dot{P})$ for calculating N_{psr} since the statistical errors there were quite acceptable.] Figure 10 shows the calculated current $\bar{J}(P_1, P_2)$ for the four cases. The current in each bin corresponds to choosing P_1 and P_2 to be the lower and upper end of the range of P in that bin. The error bars correspond to 1 σ limits, calculated in a manner similar to equation (5.3). The ranges of the bins were selected in order to have as much resolution as possible along the P axis without being swamped by the statistical noise. The range $P < 0.15$ s was eliminated because selection effects are strongest here, and it was not clear that these had been allowed for adequately.

In all the figures, the current has a maximum in the period range extending from $P \approx 0.5$ –0.7 s to $P \approx 1.5$ –2.0 s. Choosing the range of P corresponding to the maximum in \bar{J} , and assuming that this range extends from P_b to P_d as discussed in § II, we can estimate the birthrate of pulsars through equation (2.11). The results are listed in Table 2. The four estimates of birthrate range from one pulsar in ~ 20 yr to one in ~ 60 yr, the preferred estimate being

$$\text{BR}_{\text{tot}} = 1 \text{ pulsar in } \sim 56 \pm 9 \text{ yr}, \quad (5.8)$$

TABLE 2
ESTIMATES OF TOTAL AND LOCAL PULSAR BIRTHRATE IN THE GALAXY

Beaming Factor	Scale Factor	P_b (s)	P_d (s)	Birthrate
$f(P)$	$\mathcal{S}(P, L)$	0.7	2.0	$0.034 \pm 0.025 \text{ yr}^{-1}$
	$\mathcal{S}(P, \dot{P})$	0.5	1.6	$0.018 \pm 0.003 \text{ yr}^{-1}$
0.2	$\mathcal{S}(P, L)$	0.7	2.0	$0.050 \pm 0.037 \text{ yr}^{-1}$
	$\mathcal{S}(P, \dot{P})$	0.5	1.6	$0.029 \pm 0.004 \text{ yr}^{-1}$
$f(P)$	$\mathcal{S}_{\text{loc}}(P, L)$	0.7	2.0	$(3.4 \pm 2.5) \times 10^{-5} \text{ yr}^{-1} \text{ kpc}^{-2}$
	$\mathcal{S}_{\text{loc}}(P, \dot{P})$	0.5	1.6	$(1.2 \pm 0.6) \times 10^{-5} \text{ yr}^{-1} \text{ kpc}^{-2}$

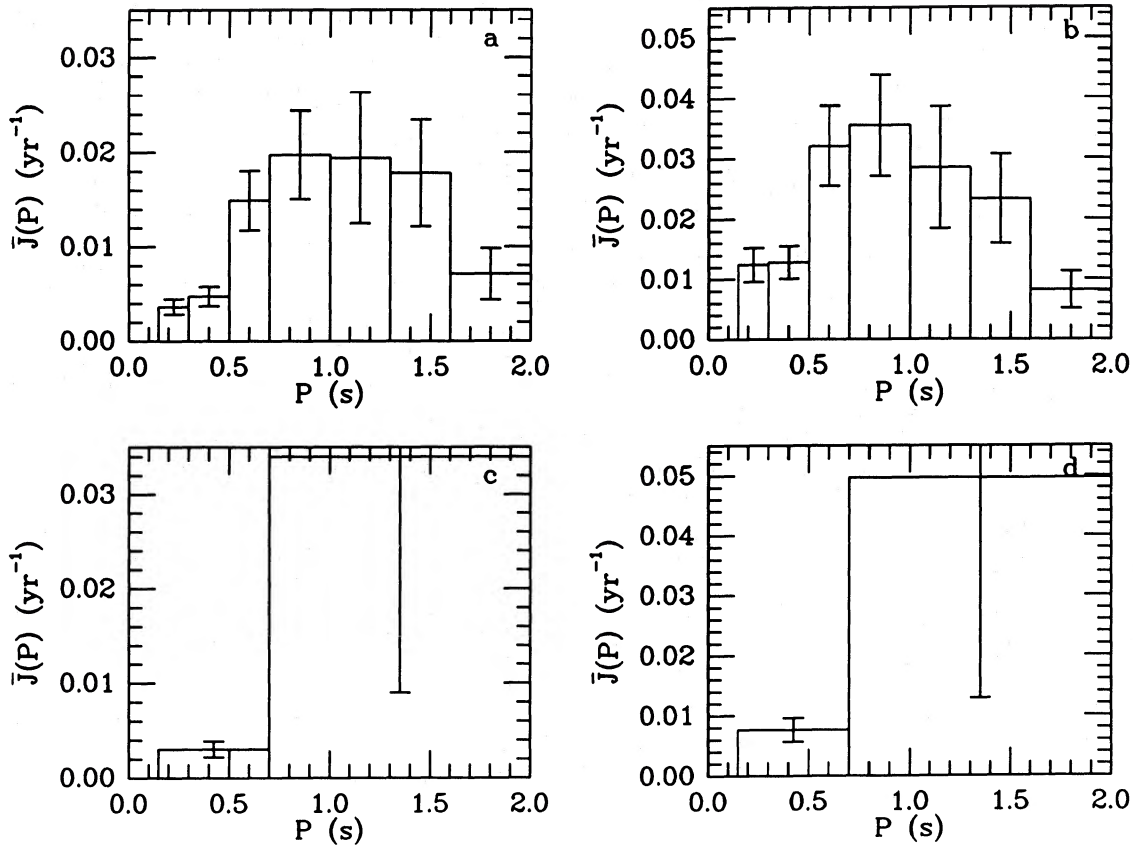


FIG. 10.—(a) Pulsar current \bar{J} estimated using the luminosity model scales $\mathcal{S}(P, \dot{P})$ and the variable beaming factor $f(P)$ of Fig. 1. (b) With $\mathcal{S}(P, \dot{P})$ and a constant beaming factor $f = 0.2$. (c) With the model-independent scales $\mathcal{S}(P, L)$ and $f(P)$. (d) With $\mathcal{S}(P, L)$ and $f = 0.2$.

obtained using $f(P)$ and $\mathcal{S}(P, \dot{P})$. The values obtained with $\mathcal{S}(P, L)$ and $\mathcal{S}(P, \dot{P})$ are consistent with each other, but the former has significantly larger statistical errors, as expected. Also, the birthrate estimates with variable $f(P)$ are smaller by $\sim 35\%$ than those with constant $f = 0.2$, just as with the estimates of N_{psr} .

A local areal pulsar current $\bar{J}_{\text{loc}}(P_1, P_2)$ in the solar vicinity was also calculated, using the local scales $\mathcal{S}_{\text{loc}}(P, L)$ and derived $\mathcal{S}_{\text{loc}}(P, \dot{P})$. The results are shown in Figure 11 and Table 2. Our best estimate of a local areal pulsar birthrate is

$$\text{BR}_{\text{loc}} = 1 \text{ pulsar per } \sim 9_{-3}^{+10} \times 10^4 \text{ yr kpc}^{-2}. \quad (5.9)$$

This is somewhat lower than the estimate of Blaauw (1985), who gives $\text{BR}_{\text{loc}} = \text{one pulsar per } \sim (4 \pm 2) \times 10^4 \text{ yr kpc}^{-2}$. Blaauw has made the important point that a comparison between the *local* pulsar birthrate and the *local* rate of formation/death of massive stars might tightly constrain the mass range of pulsar progenitors.

We come now to an effect that was highlighted by VN. All the cases in Figures 10 and 11 show that the pulsar current reaches its peak only at periods ≥ 0.5 s, implying that many pulsars are born with such long periods. This surprising result contradicts the

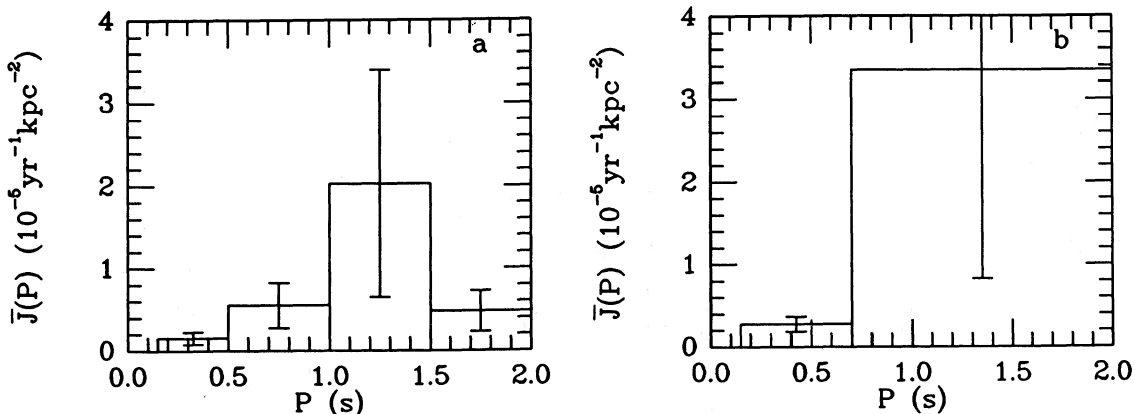


FIG. 11.—(a) Local pulsar current \bar{J} in the solar vicinity with $\mathcal{S}(P, \dot{P})$ and $f(P)$. (b) With $\mathcal{S}(P, L)$ and $f(P)$.

usual picture that pulsars are born with initial periods $P_i \approx 10$ ms. VN named this phenomenon “injection,” since pulsars are apparently being “injected” midstream into the pulsar “current.” The first reaction to the effect is that there may be some selection effect which has not been included in the calculation. Several suggestions have been made as to possible sources of error. Dewey *et al.* (1984) pointed out that VN had not allowed for the finite sampling time (τ_{samp} in § III) of the surveys. Vivekanand, Narayan, and Radhakrishnan (1982) considered the effect of dispersion smearing, while Manchester, D’Amico, and Tuohy (1985) argued that scatter-broadening would be important. All these effects have been included in the present calculation (see eq. [3.4]), and “injection” evidently survives with high significance. As further confirmation, we see that “injection” is present even in the local current calculation, which is restricted to nearby pulsars for which dispersion and scatter-broadening are negligible. Another suspect could be the luminosity model, which might overestimate the luminosity of fast pulsars, assuming thereby that they are visible over a larger fraction of the Galaxy than in reality. We test and reject this possibility in § VI. Also, note that “injection” is present even with the calculation using $\mathcal{S}(P, L)$, where no luminosity model is assumed.

The existence of “injection” implies that a large fraction of radio pulsars are born spinning rather slowly. This is in conflict with the usual assumption that (1) the material in the core of the progenitor star retains the angular momentum it had at the birth of the star because of the so-called μ -barriers that prevent the transport of angular momentum (e.g., Fricke and Kippenhahn 1972), and that (2) this angular momentum is conserved during collapse. Such a picture leads to an initial period $P_i \lesssim 1$ ms (e.g., Hardorp 1974). To explain $P_i \gtrsim 0.5$ s, the stellar core must lose nearly all its angular momentum before becoming a pulsar. It is possible that the core couples in some way to the outer layers of the presupernova star, or the ejecta during the supernova explosion. Magnetic coupling is a strong possibility, and so we study injection as a function of the pulsar magnetic field.

Magnetic fields B were estimated through the dipole braking formula, equation (4.3), and the pulsars were divided into two groups—high- B and low- B . Figure 12 shows the variation of pulsar current with P for the two groups. “Injection” is seen to be very pronounced in the high- B sample and virtually absent in the low- B sample. This would appear to rule out any P -dependent selection effect as the cause of “injection,” since the selection effect would have to depend on \dot{P} , which is extremely unlikely. It seems more reasonable to accept that “injection” is a real effect and that it is tied in some way to the pulsar magnetic field.

VI. DISCUSSION

Based on the analysis presented in this paper, our best estimate of the Galactic pulsar birthrate is one pulsar in ~ 56 yr. This rate is significantly lower than the estimates of a few years back, but it is consistent with more recent conclusions (Vivekanand 1984; LMT). Three effects have contributed to the reduction in birthrate: 1. The inclusion of the luminosity selection effect (inverse

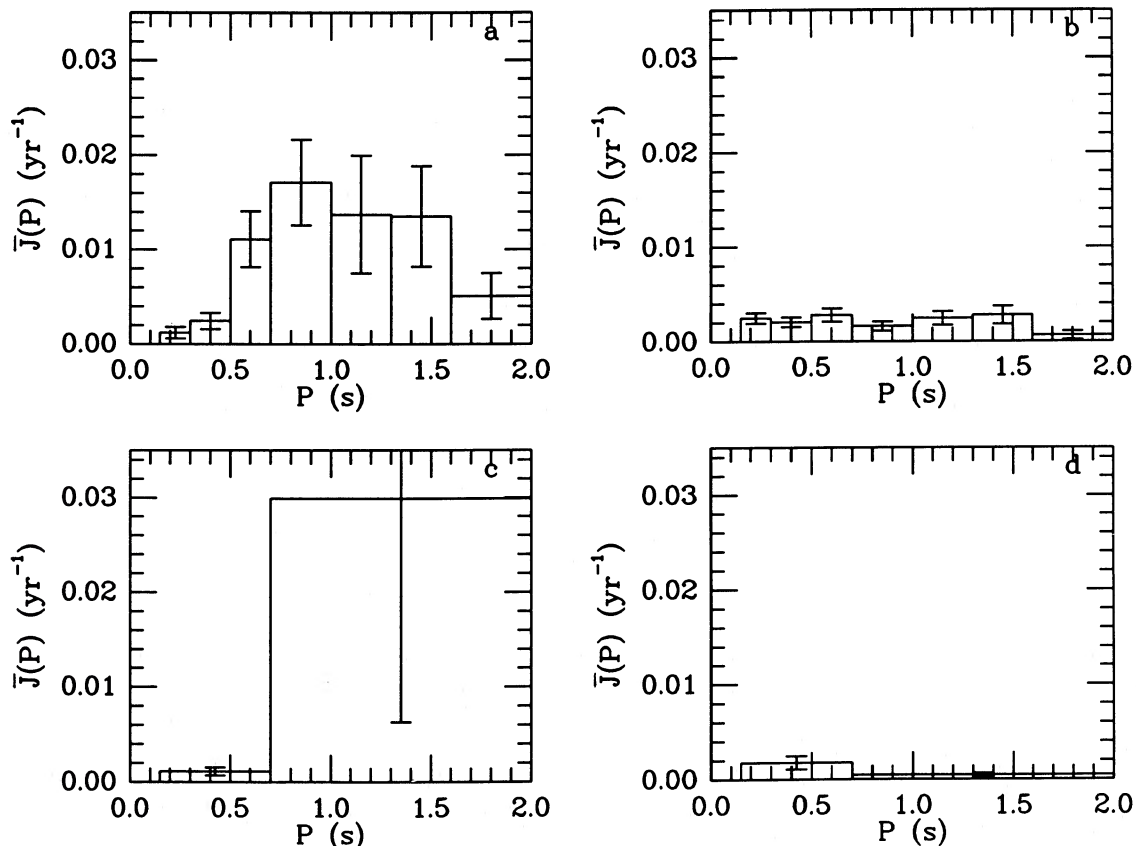


FIG. 12.—(a) Pulsar current \bar{J} for pulsars with $\log B > 12.1$ calculated using $\mathcal{S}(P, \dot{P})$ and $f(P)$. (b) $\log B < 12.1$, $\mathcal{S}(P, \dot{P})$, $f(P)$. (c) $\log B > 12.1$, with $\mathcal{S}(P, L)$ and $f(P)$. (d) $\log B < 12.1$, $\mathcal{S}(P, L)$, $f(P)$.

correlation of L with P) reduces the birthrate by a factor ~ 3 . 2. The inclusion of a variable beaming factor (Fig. 1) reduces the birthrate by a factor ~ 1.5 –2. 3. A modified distance scale introduced by LMT reduces the birthrate by a factor $\lesssim 1.5$.

Many selection effects were included in the present calculation, but one wonders if there may be other important effects that we are unaware of. LMT included an additional reduction in the birthrate by a factor of 1.5 to allow for errors in distance estimates. (There is a similar effect from luminosity variability.) This is, however, cancelled by yet another effect that we have ignored. In estimating the sensitivity limits of the four surveys, we have been liberal and used a somewhat lower value of βS_0 than indicated by the data (see Fig. 4). This was done so that enough pulsars would survive in the data base to provide reasonable statistics. However, it means that at the low flux end there are more pulsars in the Galaxy than we estimate, and so our birthrate estimate will need to be revised upward.

The discussion in § II indicated that our estimate of birthrate is technically only a lower limit since the assumption that $P_d > P_b$ is not likely to be valid. There is however a mitigating circumstance. As seen in Figure 12, the pulsar birthrate is largely dominated by high- B pulsars. In fact, half the pulsar current is carried by less than 10% of high- B pulsars in the observed sample. These pulsars do not die until they reach periods ≥ 2 s. Hence, the birthrate estimates in Table 2 calculate the full contribution of these pulsars. Some low- B pulsars probably die with $P < 1$ s, due to field decay, and our birthrate calculation underestimates the contribution from these. However, since these form a minority, the overall error is probably small. Similarly, our calculation completely neglects the contribution from millisecond pulsars since these never spin down to the slow periods that we have considered. However, most millisecond pulsars appear to be in binaries, which are not considered in this paper, and in any case their birthrate appears to be significantly lower than that for single pulsars (Narayan 1987).

Since the birthrate estimate is dominated by a few observed high- B pulsars, a serious worry is whether there could be a population of pulsars with still higher B that is missing in the observed sample. This issue was raised by Phinney and Blandford (1981) who showed that the number of pulsars falls off rather slowly as a function of \dot{P} and suggested that the integral of birthrate over \dot{P} may not converge. To assess the importance of this, we have calculated the birthrate as a function of magnetic field. For each pulsar, the initial magnetic field B_i was calculated through the formula

$$B_i^2 = 10^{39} P \dot{P} [1 + (P/\dot{P})/t_B](G)^2, \quad (6.1)$$

where t_B is the field decay time scale. Figure 13 shows the pulsar birthrate per unit $\log B_i$ as a function of $\log B_i$ for two choices of t_B , viz., 10^7 yr (LMT) and 2×10^7 yr (Krishnamohan 1987). A power-law fit of the variation at high B_i gives for both values of t_B

$$dBR/d \log B_i \approx 0.065(10^{12} \text{ G}/B_i) \text{ yr}^{-1}, \quad B_i > 2 \times 10^{12} \text{ G}. \quad (6.2)$$

The fit of this functional form to the histograms in Figure 13 is satisfactory. The important point to note is that the integral of BR over B_i is convergent. The integral gives a total birthrate of one pulsar in ~ 71 yr, which is consistent with the other estimates obtained in this paper. If equation (6.2) is a true representation of the initial magnetic field distribution, then only about 10% of pulsars are born with fields greater than the highest fields ($\sim 10^{13.2}$ G) observed so far, and so the error from missing these is small.

An important result of this paper is the strong confirmation of pulsar “injection.” The effect is seen with all the different combinations of data analysis attempted (Fig. 10). Moreover, the correlation seen between “injection” and magnetic field strength (Fig. 12) makes any explanation in terms of a selection effect unlikely. Independent evidence in favor of “injection” has been presented by Stokes *et al.* (1985) and Chevalier and Emmering (1986). However, several other papers have argued that, although the data may be *consistent* with “injection,” they do not *require* it (e.g., Manchester, D’Amico, and Tuohy 1985; LMT; Clifton and Lyne 1986). We make an important comment on this question. Most of the pulsar current, and hence birthrate, is really associated with high magnetic field objects, i.e., pulsars with high \dot{P} . This is shown by Figure 12 and is further made clear by Figure 14 where we see that at any given P , the contribution of a pulsar to the current, viz., $\dot{P} \mathcal{S}(P, \dot{P})/f(P)$, increases rapidly with \dot{P} . Because of this effect, if “injection” were present only in the subset of high field pulsars, it could be easily missed if one gave equal weight to all observed pulsars, as is usually done. The analysis presented in this paper starts off by converting the observed sample of pulsars to a representation of the true pulsar distribution using the scale factors $\mathcal{S}(P, L)$ and $\mathcal{S}(P, \dot{P})$. These numbers are then multiplied by \dot{P} to

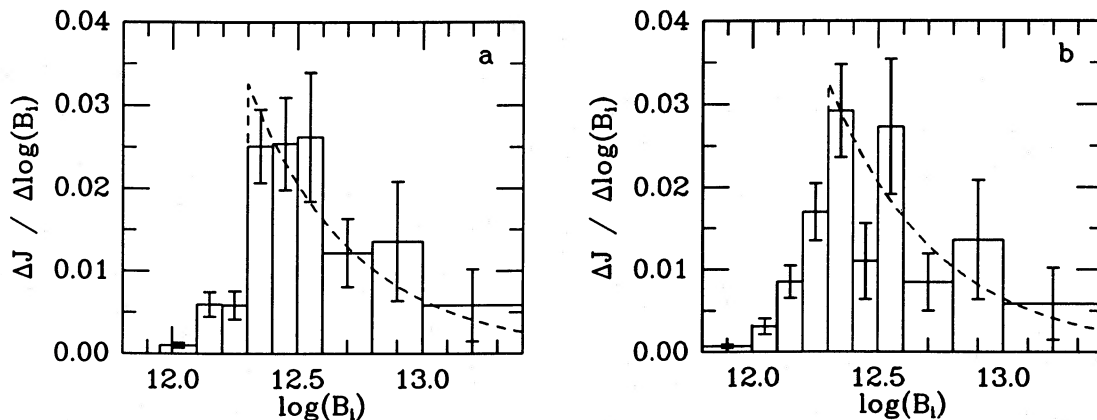


FIG. 13.—(a) Histogram of pulsar current in the period range 0.5–1.6 s as a function of initial magnetic field B_i , assuming $t_B = 10^7$ yr. (b) Same as (a), for $t_B = 2 \times 10^7$ yr. The dashed lines correspond to eq. (6.2).

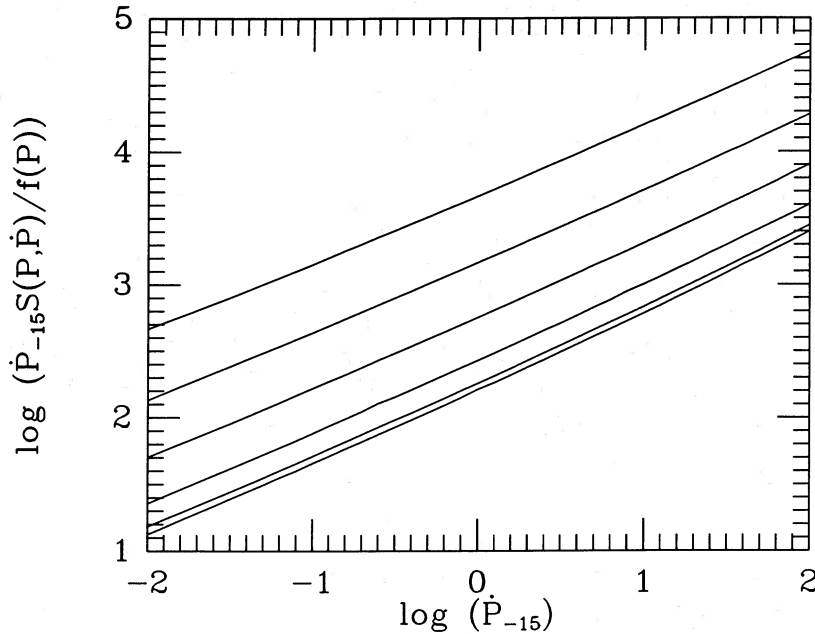


FIG. 14.—Variation of $\log [\dot{P}_{-15} \mathcal{S}(P, \dot{P}) / f(P)]$ with $\log (\dot{P}_{-15})$. Starting from the top, the curves correspond to $P = 1.6$ s, 0.8 s, 0.4 s, 0.2 s, 0.05 s, 0.1 s. The reversal in the trend at short periods is because of period-dependent selection effects.

calculate the current. The net effect is that at each P , the high- B pulsars are weighted much more strongly than the low- B pulsars (Fig. 14), and hence “injection” is seen very strikingly. We feel our approach is more appropriate when investigating questions related to the Galactic pulsar population. Other applications, such as the study of selection effects, are better carried out using the unweighted sample of observed pulsars.

A recurring theme has been the poor statistical reliability of numerical estimates, and this is particularly true of “injection.” The calculation using the scales $\mathcal{S}(P, L)$ makes no assumptions at all regarding pulsar luminosity or spin-down mechanism, but instead allows the measured luminosity of each pulsar to determine the weight of that pulsar through a V/V_{\max} -type argument. However, the evidence for “injection” in this calculation is only at the level of a couple of standard deviations. The statistics are much better when the luminosity model is introduced through the scales $\mathcal{S}(P, \dot{P})$. In this case, “injection” stands out with high significance, but one wonders if it could be an artifact introduced through the luminosity model. A look at Figure 7 shows that the model tends to overestimate pulsar luminosities at high \dot{P}/P^3 . Most of the pulsars at this end have short P , and so the effect is to underestimate the pulsar current at short P . To assess the importance of this, we have repeated the calculations with another luminosity model, shown by Figure 15. The feature of this model is that L_m is taken to be constant at high \dot{P}/P^3 , as Taylor and Stinebring (1986) and Stollman (1986) suggest. This is probably too extreme since the data do show a rising trend in this region of the figure. However, even with this luminosity model, “injection” continues to be indicated by the data, as shown in Figure 16. It would appear that an extremely drastic modification of the luminosity model will be needed before “injection” could be made to disappear. Stollman (1986) claims that no “injection” is required with the modified luminosity function; however, the comments in the previous paragraph on the importance of using the appropriate weighting function probably apply to his calculation.

Yet another selection effect may arise from the variation of pulsar scale height with period (A. G. Lyne and J. J. Goodman, private communication). It is known that fast pulsars have a smaller scale height than slow pulsars, but the results described so far assumed a common scale height for all pulsars. However, numerical calculations show that “injection” in fact becomes somewhat *stronger* when the variation of scale height is allowed for.

Summing up all the evidence, we would say that there is strong (though by no means overwhelming) evidence for “injection.” The question then is: why are many pulsars born with slow periods? We feel that the correlation between “injection” and pulsar magnetic field is an important clue, and the explanations we offer are based on this.

It is usual to assume that both angular momentum and magnetic flux are conserved during the collapse of the stellar core in a supernova explosion. Hence the initial period P_i and magnetic field B_i of a pulsar directly reflect the spin and field strength before collapse. A thorny issue in stellar physics has been the question of whether the core of a star can lose angular momentum during the life of the star. To our knowledge, this has not been settled. Convection is considered a likely source of viscosity in stellar interiors, but magnetic fields could also be important. If the dominant mechanism of angular momentum transport is magnetic coupling between the core and outer layers of the star, then it is natural to expect that stars with higher magnetic fields in their interiors would have slower rotating cores, and this could explain “injection.” The loss of angular momentum could also take place during the supernova explosion, after the neutron star has formed, but this seems less likely. The magnetic energy of a pulsar with $B \approx 10^{12.5}$ G is only $E_B \approx B^2 r^3 \approx 10^{43}$ ergs ($r \approx 10$ km is the neutron star radius), whereas the rotational energy of a pulsar with $P \approx 10$ ms is $E_{\text{rot}} \approx Mr^2 \Omega^2 \approx 10^{51}$ ergs. It is therefore hard to imagine the field having a strong dynamical influence during the short time available during a supernova explosion. (It is possible to get around this argument by saying that the magnetic field may wind up as a result of the rapid spin of the newly formed neutron star and reach a much higher field strength than $10^{12.5}$ G, thus

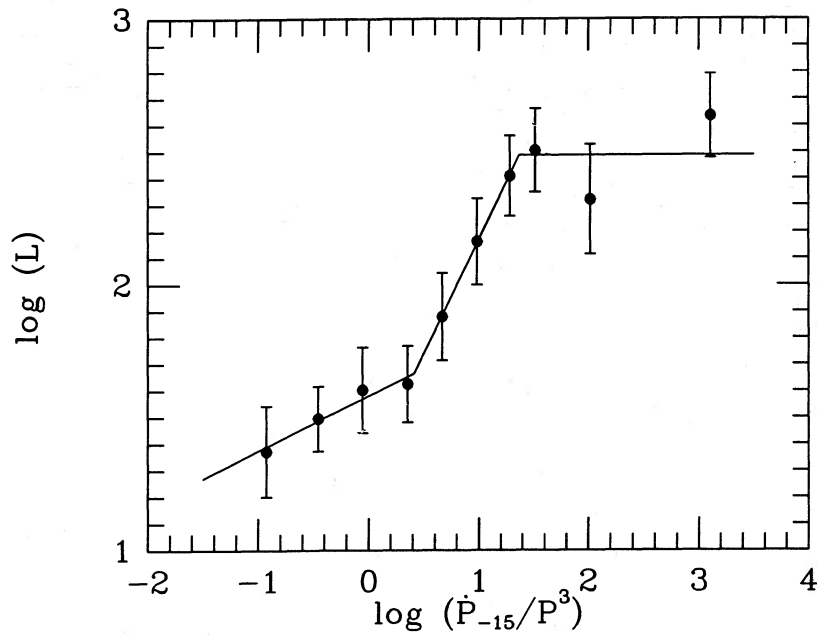


FIG. 15.—An alternative luminosity model, fitted to the same data as in Fig. 7. The model L was constrained to be constant for high values of \dot{P}_{-15}/P^3 . The other two straight line segments were adjusted so as to minimize the residuals between the model and the data.

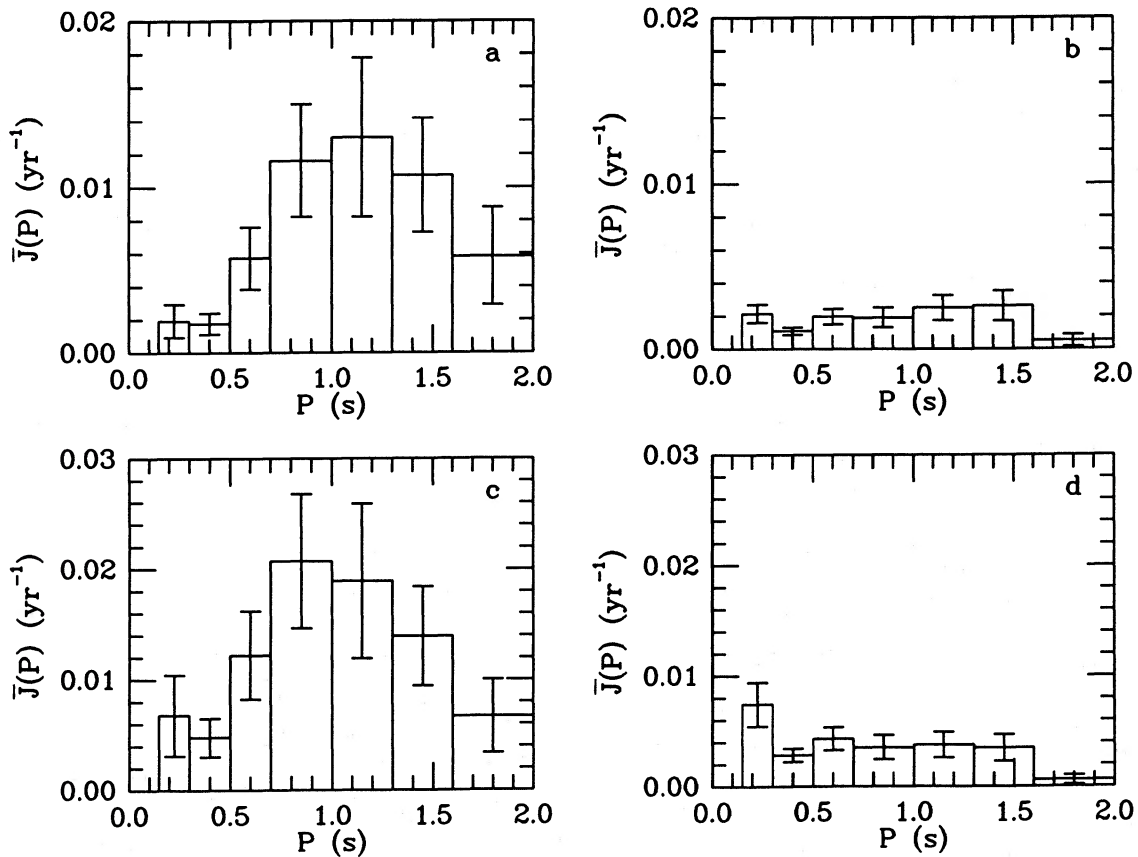


FIG. 16.—(a) Pulsar current \bar{J} for pulsars with $\log B > 12.1$ calculated with the luminosity model of Fig. 15 and using $\mathcal{S}(P, \dot{P})$ and $f(P)$. (b) $\log B < 12.1$, $\mathcal{S}(P, \dot{P})$, $f(P)$. (c) $\log B > 12.1$, $\mathcal{S}(P, \dot{P})$, $f = 0.2$. (d) $\log B < 12.1$, $\mathcal{S}(P, \dot{P})$, $f = 0.2$.

becoming dynamically important.) Since the preexplosion core is larger in radius than the neutron star by a factor $\sim 10^3$, both Ω and B would be less by $\sim 10^6$. Thus, the ratio E_B/E_{rot} would be larger by $\sim 10^3$ and the two energies would be more nearly equal. Also, any magnetic viscosity would be able to act over a much longer time, essentially the lifetime of the star. In view of the evidence for pulsar "injection," a more careful analysis of magnetic coupling and angular momentum transport in massive main-sequence stars may be worthwhile.

Another scenario that may explain "injection" is binary "recycling." Most massive stars are found in binary systems. If the asymmetry of supernova explosions is small, these systems are expected to stay bound after the first explosion. It is believed that, as the second star evolves, it transfers matter to its companion neutron star and spins up the latter. For Eddington-limited accretion, the neutron star is quickly spun up to an equilibrium period P_{eq} given by (Smarr and Blandford 1976; Srinivasan and van den Heuvel 1982)

$$P_{\text{eq}} \approx 0.9 B_{12}^{6/7} \text{ s}, \quad (6.3)$$

where $B = 10^{12} B_{12} \text{ G}$ is its dipole magnetic field. When the second star finally explodes as a supernova, the binary is disrupted, releasing a new neutron star with presumably a short period, and the "recycled" old neutron star with $P_i = P_{\text{eq}}$ (Radhakrishnan and Srinivasan 1981; Alpar *et al.* 1982; Radhakrishnan 1982). The "recycled" neutron stars would show a correlation between their magnetic fields and initial periods very similar to that indicated by the pulsar rate (although we will need to invoke super-Eddington accretion in order to fit the observed pulsar periods). In this scenario it would appear that the "injected" pulsars can form at most half of the neutron star population, whereas the pulsar data seem to require a somewhat larger fraction. One explanation could be that in the majority of binaries the second star, which is the less massive of the two, falls in the mass range $\sim 6\text{--}8 M_{\odot}$, and undergoes total disruption through degenerate carbon burning, leaving no compact remnant (Iben and Renzini 1983). Another problem with the above "recycled" neutron star scenario is that it requires most binary systems to remain bound after the first explosion. These systems would go through an X-ray phase during accretion spin-up. The birthrate of massive X-ray binaries (~ 1 in $10^{3\text{--}4}$ yr) is, however, far short of the pulsar birthrate, and it may be necessary to invoke X-ray silent accretion in most of these systems.

A third explanation of "injection" would be to invoke late switch-on of the pulsar magnetic field, in the manner suggested by Blandford, Applegate, and Hernquist (1983). In this picture, the neutron star is born with a small seed magnetic field, which is amplified by a thermoelectric phenomenon associated with the cooling flux. Thus, the neutron star is initially silent in its radio output, and switches on as a radio pulsar only after the field has grown sufficiently, by when the pulsar is spinning more slowly. If it turns out that it takes longer to generate high magnetic fields than low fields, then it would be possible to explain the correlation between "injection" and magnetic field.

Whatever may be the cause of "injection," one effect of the phenomenon is that newly born pulsars will emit more weakly in the radio than thought earlier, because of the luminosity model, equation (4.1), which has a strong dependence on the pulsar period. This could have important consequences for pulsar-supernova associations. A longstanding puzzle has been why out of over 100 shell-type supernova remnants in the Galaxy, only one (MSH 15-52) has a detected pulsar in its center. This is very hard to explain if all of these remnants had pulsars as bright as the Crab or Vela. However, if most of them contain slow, weak pulsars, the situation would be less paradoxical. A careful quantitative analysis of this question is now needed. Late switch-on of pulsars is another possibility for explaining the rarity of pulsar-supernova associations (Phinney and Blandford 1981; VN).

The author gratefully acknowledges discussions with R. D. Blandford, A. Burrows, J. M. Cordes, J. J. Goodman, S. R. Kulkarni, A. G. Lyne, J. P. Ostriker, and J. H. Taylor. Comments by the referee were very useful. This work was supported in part by the National Science Foundation under grant AST-8611121.

REFERENCES

- Alpar, M. A., Cheng, A. F., Ruderman, M. A., and Shaham, J. 1982, *Nature*, **300**, 728.
- Blaauw, A. 1985, in *Birth and Evolution of Massive Stars and Stellar Groups*, ed. W. Boland, and H. van Woerden (Dordrecht: Reidel), p. 211.
- Blandford, R., Applegate, J. H., and Hernquist, L. 1983, *M.N.R.A.S.*, **204**, 1025.
- Chevalier, R. A., and Emmering, R. T. 1986, *Ap. J.*, **304**, 140.
- Clifton, T. R., and Lyne, A. G. 1986, *Nature*, **320**, 43.
- Cordes, J. M., Weisberg, J., and Boriakoff, V. 1984, *Ap. J.*, **288**, 221.
- Damashek, M., Taylor, J. H., and Hulse, R. A. 1978, *Ap. J. (Letters)*, **225**, L31.
- Davies, J. G., Lyne, A. G., and Seiradakis, J. H. 1972, *Nature*, **240**, 229.
- Dewey, R. J., Stokes, G. H., Segelstein, D. J., Taylor, J. H., and Weisberg, J. M. 1984, in *Millisecond Pulsars*, ed. S. P. Reynolds and D. R. Stinebring (NRAO), p. 234.
- Dewey, R. J., Taylor, J. H., Weisberg, J. M., and Stokes, G. H. 1985, *Ap. J. (Letters)*, **294**, L25.
- Fricke, K. J., and Kippenhahn, R. 1972, *Ann. Rev. Astr. Ap.*, **10**, 45.
- Gunn, J. E., and Ostriker, J. P. 1970, *Ap. J.*, **160**, 979.
- Hardorp, J. 1974, *Astr. Ap.*, **32**, 133.
- Haslam, C. G. T., Salter, C. J., Stoffel, H., and Wilson, W. E. 1982, *Astr. Ap. Suppl.*, **47**, 1.
- Hulse, R. A., and Taylor, J. H. 1974, *Ap. J. (Letters)*, **191**, L59.
- Iben, I., and Renzini, A. 1983, *Ann. Rev. Astr. Ap.*, **21**, 271.
- Krishnamohan, S. 1987, in *IAU Symposium 125, The Origin and Evolution of Neutron Stars*, ed. D. J. Helfand and J. H. Huang (Dordrecht: Reidel), in press.
- Large, M. I. 1971, in *IAU Symposium 46, The Crab Nebula*, ed. R. D. Davies, and F. G. Smith (Dordrecht: Reidel), p. 165.
- Lyne, A. G. 1981, in *IAU Symposium 95, Pulsars*, ed. W. Sieber and R. Wielebinski (Dordrecht: Reidel), p. 423.
- Lyne, A. G., Manchester, R. N., and Taylor, J. H. 1985, *M.N.R.A.S.*, **213**, 613 (LMT).
- Lyne, A. G., Ritchings, R. T., and Smith, F. G. 1975, *M.N.R.A.S.*, **171**, 579.
- Manchester, R. N., D'Amico, N., and Tuohy, I. R. 1985, *M.N.R.A.S.*, **212**, 975.
- Manchester, R. N., Lyne, A. G., Taylor, J. H., Durdin, J. M., Large, M. I., and Little, A. G. 1978, *M.N.R.A.S.*, **185**, 409.
- Manchester, R. N., and Taylor, J. H. 1977, *Pulsars* (San Francisco: Freeman).
- . 1981, *A.J.*, **86**, 1953.
- Narayan, R. 1984, in *Millisecond Pulsars*, ed. S. P. Reynolds and D. R. Stinebring (NRAO), p. 279.
- . 1987, in *IAU Symposium 125, The Origin and Evolution of Neutron Stars*, ed. D. J. Helfand and J. H. Huang (Dordrecht: Reidel), in press.
- Narayan, R., and Radhakrishnan, V. 1983, *Current Sci.*, **52**, 46.
- Narayan, R., and Vivekanand, M. 1981, *Nature*, **290**, 571.
- . 1982, *Astr. Ap.*, **113**, L3.
- . 1983a, *Ap. J.*, **274**, 771.
- . 1983b, *Astr. Ap.*, **122**, 45.
- Phinney, E. S., and Blandford, R. D. 1981, *M.N.R.A.S.*, **194**, 137.
- Proszynski, M., and Przybycien, D. 1984, in *Millisecond Pulsars*, ed. S. P. Reynolds and D. R. Stinebring (NRAO), p. 151.
- Radhakrishnan, V. 1982, *Contemporary Phys.*, **23**, 207.
- Radhakrishnan, V., and Srinivasan, G. 1981, paper presented at Second Asian Pacific Regional IAU Meeting, Bandung.
- Rickett, B. J. 1978, *Ann. Rev. Astr. Ap.*, **15**, 479.
- Romani, R., Narayan, R., and Blandford, R. 1985, *M.N.R.A.S.*, **220**, 19.

- Segelstein, D. J., Rawley, L. A., Stinebring, D. R., Fruchter, A. S., and Taylor, J. H. 1986, *Nature*, **322**, 714.
- Smarr, L. L., and Blandford, R. D. 1976, *Ap. J.*, **207**, 574.
- Srinivasan G., Bhattacharya, D., and Dwarakanath, K. S. 1984, *J. Ap. Astr.*, **5**, 403.
- Srinivasan, G., and van den Heuvel, E. P. J. 1982, *Astr. Ap.*, **108**, 143.
- Stokes, G. H., Taylor, J. H., Weisberg, J. M., and Dewey, R. J. 1985, *Nature*, **317**, 787.
- Stollman, G. M. 1986, preprint.
- Taylor, J. H., and Manchester, R. N. 1977, *Ap. J.*, **215**, 885.
- Taylor, J. H., and Stinebring, D. R. 1986, *Ann. Rev. Astr. Ap.*, **24**, 285.
- Vivekanand, M. 1984, Ph.D. thesis, Bangalore University.
- Vivekanand, M., and Narayan, R. 1981, *J. Ap. Astr.*, **2**, 315 (VN).
- Vivekanand, M., Narayan, R., and Radhakrishnan, V. 1982, *J. Ap. Astr.*, **3**, 237.

RAMESH NARAYAN: Steward Observatory, University of Arizona, Tucson, AZ 85721